International Journal of Solids and Structures 47 (2010) 816–826

Contents lists available at ScienceDirect

International Journal of Solids and Structures

journal homepage: www.elsevier.com/locate/ijsolstr

Surface waves in a piezoelectric–semiconductor composite structure

J.N. Sharma *, K.K. Sharma, Ashwani Kumar

Department of Applied Sciences, National Institute of Technology, Hamirpur 177 005, India

ARTICLE INFO

Article history:
Received 1 July 2009
Received in revised form 24 September 2009
Available online 3 December 2009

Keywords:
Semiconductor
Piezoelectricity
Life time
Acoustic waves
Dispersion

ABSTRACT

The present work deals with the propagation of interfacial surface waves in a composite consisting of homogeneous, transversely isotropic, piezoelectric halfspace underlying a thin layer of non-piezoelectric semiconductor material. The mathematical model of the problem is depicted by partial differential equations of motion for the structure and boundary conditions to be satisfied at the interface and free surface of the composite. After obtaining formal wave solution of the model the secular equation that governs the propagation of surface waves in the considered composite structure has been derived in compact form. The numerical solution of secular equation is being carried out for the composites Si–CdSe, Ge–CdSe and Ge–PZT by employing functional iteration method along with irreducible Cardano method using MATLAB programming. The computer simulated results in respect of dispersion curves, attenuation coefficient and specific loss factor of energy dissipation are presented graphically for Si–CdSe composite to illustrate the analytical developments. We have extended our analysis to Ge–CdSe and Ge–PZT composites also. However, to avoid clustering of profiles and also to have clear understanding of the variations, the computer simulated values of phase velocity and attenuation coefficient are presented in tabular form for all three considered composite structures. This work may be useful for designing and construction of surface acoustic wave (SAW) devices and electronics industry.

1. Introduction

Curie and Curie (1880) discovered the electromechanical effect in certain noncentro-symmetric crystalline materials. These materials become electrically polarized under the influence of an external applied mechanical force. Chen (1971), Chizhikov et al. (1985) and He (2001) further laid foundation to the various concepts and applications of piezoelectric and electromagnetic solids. de Lorenzi and Tierten (1975) and Maugin and Daher (1986) developed nonlinear theories for deformable semiconductors. Weinreich et al. (1959) regarded acoustoelectric effect viz. the interaction between traveling wave and mobile charges in a piezoelectric semiconductor, as wave particle drag. Hutson and White (1962) studied the dispersion and acoustic losses in the crystals having semiconducting properties in addition to their piezoelectric character.

It is a well-known fact that the surface and bulk acoustic waves can be generated in piezoelectric materials under the effect of electromechanical and thermal fields. White (1962) predicted that an acoustic wave propagating in a piezoelectric semiconductor can be amplified under the effect of a DC electric field. Collins et al. (1968) observed strong interaction between the wave on the surface of piezoelectric crystal and the wave on the drifting carriers in the nearby semiconductor. Dietz et al. (1988) explored the acoustoelectric amplification of acoustic waves in the composite of piezoelectric dielectric and non-piezoelectric semiconductor. White (1967) discussed the phenomena surface elastic wave propagation, transduction and amplification in a piezoelectric semiconductor with special emphasis on the characteristics useful in electronic devices. The acoustoelectric amplification in a piezoelectric coated with semiconductor film was analyzed by the authors: Fischler and Yando (1969), Fischler (1970), Kino and Reeder (1971). Yang and Zhou (2004, 2005) found that the phenomenon of semiconduction leads to dispersion and acoustic losses in piezoelectric surface waves generated in the piezoelectric semiconductors. Sharma and Pal (2004) investigated the propagation of Lamb waves in a homogeneous, transversely isotropic, piezothermoelastic plate. Sharma et al. (2005) studied the propagation of thermoelastic Rayleigh waves in piezothermoelastic materials. Sharma and Walia (2007) carried out further investigations on the propagation of Rayleigh waves in a homogeneous, transversely isotropic, piezothermoelastic semi-space.

Maruszewski (1989) considered the interactions between elastic, thermal and charge carrier's field in semiconductors and found the existence of two kinds of waves namely, elastic longitudinal and transverse waves of Rayleigh type in addition to electron longitudinal waves. Sharma and Thakur (2006) studied the plane harmonic elasto-thermodiffusive waves in semiconductors. It has been noticed that the shear waves get decoupled from rest of the

* Corresponding author. Tel.: +91 1972 223296; fax: +91 1972 223834.
E-mail addresses: jns@nitham.ac.in (J.N. Sharma), kks@nitham.ac.in (K.K. Sharma), puri_nit@yahoo.com (A. Kumar).

0020-7683/$ - see front matter © 2009 Elsevier Ltd. All rights reserved.
doi:10.1016/j.ijsolstr.2009.11.016

motion and are not affected by the other fields. According to the frequency equation, four coupled longitudinal waves, namely quasi-thermoelastic (QTN), elastodiffusive (QEN/QEP), thermodiffusive (QTN/QTP) and quasi-thermal (T-mode) can be propagated in an infinite semiconductor. Sharma et al. (2007, 2009) also investigated the elasto-thermodiffusive wave propagation on semiconductor materials and observed that the life time of charge carriers and thermal relaxation time affect the wave characteristics significantly. It has been observed that at long wavelengths, the material exhibit more internal friction with increasing life time of charge carrier field. Sharma et al. (2008) investigated the propagation of elasto-thermodiffusive surface waves under the effect of thermal field in a semiconductor halfspace underlying a fluid. They concluded that the phase velocity, attenuation coefficient of leaky Rayleigh waves (LRWs) and non-leaky Rayleigh waves (NLRWs) are significantly affected by the thickness and temperature of fluid loading, relaxation and life times of carrier field.

Keeping in view the above work we in this paper have made an attempt to study the effect of n-type semiconductor layer on a homogeneous transversely isotropic, 6 mm class piezoelectric halfspace on the wave characteristics such as phase velocity, attenuation coefficient and specific loss factor of the energy dissipation of waves at the interface of the structure. The effect of life time of the carrier field on the wave propagation for different modes of vibration has also been investigated to explore the interaction between the surface waves and the carrier field. Some special cases of wave propagation in a piezoelectric halfspace subjected to charge free (open circuit) and electrically shorted (closed circuit) boundary conditions have also been deduced and studied.

2. Formulation of the problem

We consider a homogeneous transversely isotropic, piezoelectric halfspace whose surface is coated with a thin layer of non-piezoelectric elastic semiconductor of thickness 'h' as shown in Fig. 1. We take the origin of coordinate system $oxyz$ at any point on the plane surface (interface) and z-axis pointing vertically downward into the piezoelectric halfspace. Thus, the piezoelectric semi-space is represented by $z \geqslant 0$ and the semiconductor layer occupies the region $0 \leqslant z \leqslant -h$. We choose x-axis along the direction of wave propagation in such a way that all particles on the line parallel to y-axis are equally displaced. Therefore, all field quantities are independent of y-coordinate.

Further, the disturbance is assumed to be confined in the neighborhood of the interface $z = 0$, and hence vanishes as $z \to \infty$. The basic governing equations of motion and electron diffusion for the composite structure under study, in the absence of body forces and electric sources, are given below:

(i) Homogeneous isotropic, n-type semiconductor elastic layer (Sharma et al., 2007; Maruszewski, 1989):

$$\mu\nabla^2\vec{u}^s + (\lambda+\mu)\nabla\nabla\cdot\vec{u}^s - \lambda^n\nabla N = \rho^s\ddot{\vec{u}}^s \tag{1}$$

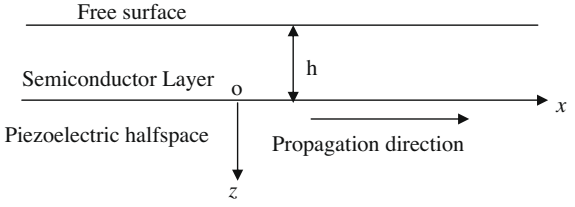

Fig. 1. Geometry of the problem.

$$\rho^s D^n\nabla^2 N - \rho^s\left(1+t^n\frac{\partial}{\partial t}\right)\dot{N} - a_2^n T_0\lambda^T\nabla\cdot\dot{\vec{u}}^s = -\left(1+t^n\frac{\partial}{\partial t}\right)\left(\frac{\rho^s}{t_n^+}\right)N \tag{2}$$

(ii) Transversely isotropic piezoelectric (6 mm class) medium (Sharma and Pal, 2004):

$$c_{11}u^p_{,xx} + c_{44}u^p_{,xz} + (c_{13}+c_{44})w^p_{,xz} + (e_{15}+e_{31})\phi^p_{,xz} = \rho^p\ddot{u}^p \tag{3}$$

$$(c_{13}+c_{44})u^p_{,xz} + c_{44}w^p_{,xx} + c_{33}w^p_{,zz} + e_{15}\phi^p_{,xx} + e_{33}\phi^p_{,zz} = \rho^p\ddot{w}^p \tag{4}$$

$$(e_{15}+e_{31})u^p_{,xz} + e_{15}w^p_{,xx} + e_{33}w^p_{,zz} - \varepsilon_{11}\phi^p_{,xx} - \varepsilon_{33}\phi^p_{,zz} = 0 \tag{5}$$

where the notations $\nabla^2 = \frac{\partial^2}{\partial x^2} + \frac{\partial^2}{\partial z^2}$, $N = n - n_0$, $a_2^n = \frac{a^{Qp}}{a^Q}$, $\lambda^T = (3\lambda+2\mu)\alpha_T$ have been used. In the above equations, the superposed dots on various quantities denote time differentiation and comma notation is used for spatial derivatives. Throughout this paper the superscripts p, s on the field quantities and material parameters refers to piezoelectric and semiconductor materials, respectively. Here λ, μ are Lamè's parameters; ρ^s is the density; λ^n is the elastodiffusive constants of electrons; D^n is the diffusion coefficient of electron; t_n^+ and t^n are the life time and relaxation time of the carriers fields; n_0 and n are the equilibrium and non-equilibrium values of electrons concentration; α_T is the coefficient of linear thermal expansion of the semiconductor material. The quantities a^{Qp}, a^Q are flux-like constants and T_0 is the uniform temperature; $\vec{u}^s = (u^s, 0, w^s)$ and $\vec{u}^p = (u^p, 0, w^p)$ are displacement vectors for semiconductor and of piezoelectric materials, respectively. The quantities ϕ^p, ρ^p, c_{ij} and e_{ij} are the electric potential, density, elastic parameters and piezoelectric constants; ε_{11} and ε_{33} are the electric permittivities perpendicular and along the axis of symmetry of piezoelectric material, respectively.

The non-vanishing components of stresses, current density and electric displacement in both the media are:

$$\begin{aligned}
\tau^s_{zz} &= (\lambda+2\mu)\frac{\partial w^s}{\partial z} + \lambda\frac{\partial u^s}{\partial x} - \lambda^n N,\\
\tau^s_{xz} &= \mu\left(\frac{\partial u^s}{\partial z} + \frac{\partial w^s}{\partial x}\right),\\
J^s_z &= -eD^n N_{,z}
\end{aligned} \tag{6}$$

for semiconductor medium and

$$\begin{aligned}
\tau^p_{zz} &= c_{13}\frac{\partial u^p}{\partial x} + c_{33}\frac{\partial w^p}{\partial z} + e_{33}\frac{\partial\phi^p}{\partial z},\\
\tau^p_{xz} &= \frac{c_{44}}{2}\left(\frac{\partial u^p}{\partial z} + \frac{\partial w^p}{\partial x}\right) + e_{15}\frac{\partial\phi^p}{\partial x},\\
D^p_z &= e_{31}\frac{\partial u^p}{\partial x} + e_{33}\frac{\partial w^p}{\partial z} - \varepsilon_{33}\frac{\partial\phi^p}{\partial z}
\end{aligned} \tag{7}$$

for piezoelectric material. Here τ^s_{ij} and τ^p_{ij} are the stress tensors. The quantities J^s_z and $N_{,z}$, respectively, denote the current density and carrier density gradient in semiconducting layer; D^p_z is the electric displacement vector of piezoelectric material and e is the electronic charge.

2.1. Boundary conditions

The requirement of continuity of stresses, displacements, electric fields and current density at the interface ($z = 0$) of two media leads to the following interfacial boundary conditions:

$$\tau^p_{zz} = \tau^s_{zz}, \quad \tau^p_{xz} = \tau^s_{xz}, \quad u^p = u^s, \quad w^p = w^s, \quad \phi^p = N, \quad D^p_z = J^s_z \tag{8}$$

Also the surface ($z=-h$) of the semiconductor is assumed to be stress free and impermeable which leads to the conditions

$$\tau^s_{zz}=0,\quad \tau^s_{xz}=0,\quad N_{,z}=0 \tag{9}$$

In order to simplify the above model, we define following quantities:

$$x'=\frac{\omega^* x}{v_l},\quad z'=\frac{\omega^* z}{v_l},\quad t'=\omega^* t,\quad t^{n'}=\omega^* t^n,\quad t_n^{+'}=\omega^* t_n^+,$$
$$N'=\frac{N}{n_0},\quad D_z^{p'}=\frac{\rho^s v_l^2}{\lambda^n n_0 e_{33}}D_z^p,\quad u^{s'}=\frac{\rho^s\omega^* v_l}{\lambda^n n_0}u^s,\quad w^{s'}=\frac{\rho^s\omega^* v_l}{\lambda^n n_0}w^s,$$
$$u^{p'}=\frac{\rho^s\omega^* v_l}{\lambda^n n_0}u^p,\quad w^{p'}=\frac{\rho^s\omega^* v_l}{\lambda^n n_0}w^p,\quad \tau_{ij}^{p'}=\frac{\tau_{ij}^p}{\lambda^n n_0},\quad \tau_{ij}^{s'}=\frac{\tau_{ij}^s}{\lambda^n n_0},$$
$$J_z^{s'}=\frac{J_z^s}{en_0 v_l},\quad c_1=\frac{c_{33}}{c_{11}},\quad c_2=\frac{c_{44}}{c_{11}},\quad c_3=\frac{c_{13}+c_{44}}{c_{11}},$$
$$e_1=\frac{e_{15}+e_{31}}{e_{33}},\quad v_l^2=\frac{\lambda+2\mu}{\rho^s},\quad e_2=\frac{e_{15}}{e_{33}},\quad \bar\varepsilon=\frac{\varepsilon_{11}}{\varepsilon_{33}},$$
$$\eta_3=\frac{\varepsilon_{33}c_{11}}{e_{33}^2},\quad \omega'=\frac{\omega}{\omega^*},\quad c'=\frac{c}{v_l},\quad v_p=\sqrt{\frac{c_{11}}{\rho^p}},\quad \bar\rho=\frac{\rho^p}{\rho^s},$$
$$\bar\lambda_n=\frac{\lambda^n n_0}{\lambda^T T_0},\quad \delta_1^2=\frac{v_l^2}{v_p^2},\quad \phi^{p'}=\varepsilon_p\phi^p,\quad \varepsilon_p=\frac{e_{33}\omega^*\rho^s v_l}{c_{11}\lambda^n n_0},$$
$$\varepsilon_n=\frac{a_2^n\lambda^{T^2}T_0\bar\lambda_n}{\rho^s(\lambda+2\mu)n_0},\quad \omega^*=\frac{v_l^2}{D^n},\quad \delta^2=\frac{v_t^2}{v_l^2},\quad v_t^2=\frac{\mu}{\rho^s} \tag{10}$$

where ω^* is the characteristic frequency, and v_l, v_t are, respectively, the longitudinal and shear wave velocities.

On substituting the quantities (10) in Eqs. (1)–(7), we obtain

$$\delta^2\nabla^2\vec u^s+(1-\delta^2)\nabla\nabla\cdot\vec u^s-\nabla N=\ddot{\vec u}^s \tag{11}$$

$$\nabla^2 N-\left[-\frac{1}{t_n^+}+\left(1-\frac{t^n}{t_n^+}\right)\frac{\partial}{\partial t}+t^n\frac{\partial^2}{\partial t^2}\right]N-\varepsilon_n\nabla\cdot\ddot{\vec u}^s=0 \tag{12}$$

$$u^p_{,xx}+c_2u^p_{,xz}+c_3w^p_{,xz}+e_1\phi^p_{,xz}=\delta_1^2\ddot u^p \tag{13}$$

$$c_3u^p_{,xz}+c_2w^p_{,xx}+c_1w^p_{,zz}+e_2\phi^p_{,xx}+\phi^p_{,zz}=\delta_1^2\ddot w^p \tag{14}$$

$$e_1u^p_{,xz}+e_2w^p_{,xx}+w^p_{,zz}-\eta_3\bar\varepsilon\phi^p_{,xx}-\eta_3\phi^p_{,zz}=0 \tag{15}$$

$$\tau^s_{zz}=(1-2\delta^2)\frac{\partial u^s}{\partial x}+\frac{\partial w^s}{\partial z}-N,\quad \tau^s_{xz}=\delta^2\left(\frac{\partial u^s}{\partial z}+\frac{\partial w^s}{\partial x}\right),\quad J_z^s=-N_{,z} \tag{16}$$

$$\tau^p_{xx}=\frac{\bar\rho}{\delta_1^2}\left\{(c_3-c_2)\frac{\partial u^p}{\partial x}+c_1\frac{\partial w^p}{\partial z}+\phi^p_{,z}\right\},$$
$$\tau^p_{xz}=\frac{\bar\rho}{\delta_1^2}\left\{\frac{c_2}{2}\left(\frac{\partial u^p}{\partial z}+\frac{\partial w^p}{\partial x}\right)+e_2\phi^p_{,x}\right\},$$
$$D_z^p=(e_1-e_2)\frac{\partial u^p}{\partial x}+\frac{\partial w^p}{\partial z}-\eta_3\phi^p_{,z} \tag{17}$$

We introduce the scalar and vector point potential functions ϕ^s and ψ^s through the relations

$$u^s=\frac{\partial\phi^s}{\partial x}+\frac{\partial\psi^s}{\partial z},\quad w^s=\frac{\partial\phi^s}{\partial z}-\frac{\partial\psi^s}{\partial x} \tag{18}$$

to facilitate the solutions in semiconductor layer

Using relations (18) in Eqs. (11) and (12), we obtain

$$\nabla^2\phi^s-N-\ddot\phi^s=0 \tag{19}$$

$$\nabla^2\psi^s=\frac{\ddot\psi^s}{\delta^2} \tag{20}$$

$$\nabla^2 N-\left[-\frac{1}{t_n^+}+\left(1+\frac{t^n}{t_n^+}\right)\frac{\partial}{\partial t}+t^n\frac{\partial^2}{\partial t^2}\right]N-\varepsilon_n\nabla^2\dot\phi^s=0 \tag{21}$$

Eq. (20) corresponds to purely transverse waves in the semiconductor which get decoupled from rest of the motion and are not affected by the charge carrier fields.

3. Formal solution of the problem

We assume the harmonic wave solution of the form

$$(\psi^s,\phi^s,N,u^p,w^p,\phi^p)=(\bar\psi^s,\bar\phi^s,\bar N,\bar u^p,\bar w^p,\bar\phi^p)\exp\{ik(x-ct)\} \tag{22}$$

where $c=\frac{\omega}{k}$ is the phase velocity, k, ω are, respectively, the wave number and angular frequency.

Upon using solution (22) in Eqs. 13, 14, 15 and 19, 20, 21, the straightforward algebraic simplifications leads to the following formal solutions satisfying the radiation condition in both the media:

(i) Semiconductor (n-type) layer $0\leqslant z\leqslant -h$:

$$\psi^s=\left(A_3^s e^{\beta z}+B_3^s e^{-\beta z}\right)\exp\{ik(x-ct)\} \tag{23}$$

$$(\phi^s,N)=\sum_{i=1}^{2}(1,S_i)\left(A_i^s e^{n_i z}+B_i^s e^{-n_i z}\right)\exp\{ik(x-ct)\} \tag{24}$$

(ii) Piezoelectric (6 mm class) halfspace ($z\geqslant 0$):

$$(u^p,w^p,\phi^p)=\sum_{i=1}^{3}(1,M_i,P_i)A_i^p\exp\{-m_i z+ik(x-ct)\} \tag{25}$$

where

$$\alpha^2=k^2(1-c^2),\quad S_i=n_i^2-\alpha^2,\quad n_i^2=k^2\left(1-c^2a_i^2\right),\ i=1,2,$$
$$\beta^2=k^2\left(1-\frac{c^2}{\delta^2}\right),\quad \xi=\left(1-\delta_1^2c^2\right) \tag{26}$$

$$A=\left(c_1\bar\varepsilon+c_2-\delta_1^2c^2\right)\eta_3+2e_2,\quad B=\left(c_2-\delta_1^2c^2\right)\eta_3\bar\varepsilon+e_2^2,$$
$$a_1^2+a_2^2=1+t^n+i\omega^{-1}\left(1+\varepsilon_n-\frac{t^n}{t_n^+}\right)+\frac{1}{\omega^2t_n^+},$$
$$a_1^2a_2^2=t^n+i\omega^{-1}\left(1-\frac{t^n}{t_n^+}\right)+\frac{1}{\omega^2t_n^+} \tag{27}$$

$$m_1^2+m_2^2+m_3^2=k^2\frac{\{c_2A+\xi(1+\eta_3c_1)-c_3(c_3\eta_3+2e_1)+c_1e_1^2\}}{c_2(1+\eta_3c_1)},$$
$$m_1^2m_2^2+m_2^2m_3^2+m_3^2m_1^2=k^4\frac{\{c_2B+\xi A-c_3(c_2\eta_3\bar\varepsilon+2e_1e_2)+e_1^2(c_2-\delta_1^2c^2)\}}{c_2(1+\eta_3c_1)},$$
$$m_1^2m_2^2m_3^2=k^6\frac{\xi B}{c_2(1+\eta_3c_1)} \tag{28}$$

$$M_i=\frac{ikm_i\left\{c_3\eta_3\left(m_i^2-k^2\bar\varepsilon\right)+e_1\left(m_i^2-k^2e_2\right)\right\}}{\left(c_1m_i^2-k^2c_2+\delta_1^2k^2c^2\right)\left(m_i^2-k^2\bar\varepsilon\right)\eta_3+\left(m_i^2-k^2e_2\right)^2},$$
$$i=1,2,3 \tag{29}$$

$$P_i=\frac{-ike_1m_i}{\eta_3\left(m_i^2-k^2\bar\varepsilon\right)}+\frac{\left(m_i^2-k^2e_2\right)}{\eta_3\left(m_i^2-k^2\bar\varepsilon\right)}M_i,\quad i=1,2,3 \tag{30}$$

Substituting the solutions (23) and (24) in Eqs. (16) and (18), we obtain the normal stress, shear stress, current density and displacements for the semiconductor material as:

$$\tau_{zz}^s = \left\{ p\sum_{i-1}^{2}\left(A_i^s e^{n_i z} + B_i^s e^{-n_i z}\right) - q\beta\left(A_3^s e^{\beta z} - B_3^s e^{-\beta z}\right)\right\}\exp\{ik(x-ct)\} \tag{31}$$

$$\tau_{xz}^s = \left\{ q\sum_{i-1}^{2} n_i\left(A_i^s e^{n_i z} - B_i^s e^{-n_i z}\right) + p\left(A_3^s e^{\beta z} + B_3^s e^{-\beta z}\right)\right\}\exp\{ik(x-ct)\} \tag{32}$$

$$J_z^s = -\sum_{i=1}^{2} S_i n_i\left(A_i^s e^{n_i z} - B_i^s e^{-n_i z}\right)\exp\{ik(x-ct)\} \tag{33}$$

$$u^s = \left\{ \frac{q}{2}\sum_{i=1}^{2}\left(A_i^s e^{n_i z} + B_i^s e^{-n_i z}\right) + \beta\left(A_3^s e^{\beta z} - B_3^s e^{-\beta z}\right)\right\}\exp\{ik(x-ct)\} \tag{34}$$

$$w^s = \left\{ \sum_{i-1}^{2} n_i\left(A_i^s e^{n_i z} - B_i^s e^{-n_i z}\right) - \frac{q}{2}\left(A_3^s e^{\beta z} + B_3^s e^{-\beta z}\right)\right\}\exp\{ik(x-ct)\} \tag{35}$$

where $p = (k^2+\beta^2), q = 2ik$ and $A_i^s, B_i^s(1,2)$ are the unknowns to be determine.

Similarly we obtain expressions for normal stress, shear stress and electric displacement for piezoelectric halfspace by using Eqs. (25) in (17) as:

$$\left(\tau_{zz}^p, \tau_{xz}^p, D_z^p\right) = \sum_{i=1}^{3}(y_i, d_i, b_i)A_i^p \exp\{-m_i z + ik(x-ct)\} \tag{36}$$

where

$$\begin{aligned} y_i &= \frac{\bar{\rho}}{\delta^2\delta_1^2}\{ik(c_3-c_2) - (c_1M_i + P_i)m_i\},\\ d_i &= \frac{\bar{\rho}}{\delta^2\delta_1^2}\left\{\frac{c_2}{2}(ikM_i - m_i) + ike_2P_i\right\},\\ b_i &= ik(e_1-e_2) - m_i(M_i - \eta_3 P_i), \quad i = 1,2,3 \end{aligned} \tag{37}$$

and A_i^p, $i = 1,2,3$ are the unknowns.

4. Secular equation

Considering the formal solution for various field quantities obtained in the previous section and employing the boundary conditions (8) and (9) we obtain a system of nine homogeneous algebraic equations having nine unknowns A_i^s, B_i^p and A_i^p $(i = 1,2,3)$ and these have a non-trivial solution if the determinant of the coefficient of A_i^s, B_i^s, A_i^p, $(i = 1,2,3)$ vanishes. After a lengthy algebraic reductions and simplifications we get the secular equation for the propagation of guided waves in the considered composite structure as:

$$\det(a_{ij}) = 0, \quad (i,j = 1,2,3,\ldots,7) \tag{38}$$

where the non-zero elements a_{ij} are given as

$$\begin{aligned}
&a_{12} = (iky_3 - p)g_2 + y_{32}pd_3, \quad a_{13} = -py_{32},\\
&a_{15} = -qy_{32}\delta^2, \quad a_{16} = -\beta\left\{p + \left(\frac{q^2}{2}\right)\right\},\\
&a_{17} = (y_{31}g_2 - y_{32}g_1), \quad a_{22} = (-M_3g_2 + d_3M_{23})p,\\
&a_{23} = -\left(\frac{q}{2}\right)g_2 - pM_{23}, \quad a_{25} = g_2 - qM_{23}\delta^2,\\
&a_{27} = M_{13}g_2 - M_{23}g_1, \quad a_{31} = n_1^2 - n_2^2,\\
&a_{32} = (S_2y_3 - pP_3)g_2 + pd_3P_{23},\\
&a_{33} = -pP_{23}, \quad a_{35} = -qP_{23}\delta^2, \quad a_{36} = -q\beta S_2,\\
&a_{37} = P_{13}g_2 - P_{23}g_1, \quad a_{42} = (b_3g_2 + d_3j_{32})p,\\
&a_{43} = -pj_{32}, \quad a_{44} = a_{31}, \quad a_{45} = S_2g_2 - qj_{32}\delta^2,\\
&a_{47} = j_{31}g_2 - j_{32}g_1, \quad a_{51} = p\{\cosh(n_1h) - \cosh(n_2h)\},\\
&a_{52} = py_3g_2\cosh(n_2h),\\
&a_{53} = q\beta g_2, \quad a_{54} = p\left[\left\{\frac{\sinh(n_2h)}{n_2}\right\} - \left\{\frac{\sinh(n_1h)}{n_1}\right\}\right],\\
&a_{55} = -g_2p\delta^2\frac{\sinh(n_2h)}{n_2},\\
&a_{56} = qp\beta\{\cosh(\beta h) - \cosh(n_2h)\},\\
&a_{61} = qn_2\sinh(n_2h) - qn_1\sinh(n_1h),\\
&a_{62} = -y_3qn_2g_2\sinh(n_2h), \quad a_{63} = pg_2\cosh(\beta h),\\
&a_{64} = q\{\cosh(n_1h) - \cosh(n_2h)\}, \quad a_{65} = qg_2\delta^2\cosh(n_2h),\\
&a_{66} = p^2\sinh(\beta h) - q^2\beta n_2\sinh(n_2h),\\
&a_{71} = S_2n_2\sinh(n_2h) - S_1n_1\sinh(n_1h),\\
&a_{72} = -S_2n_2y_3g_2\sinh(n_2h), \quad a_{74} = S_1\cosh(n_1h) - S_2\cosh(n_2h),\\
&a_{75} = g_2S_2\cosh(n_2h), \quad a_{76} = q\beta S_2n_2\cosh(n_2h),\\
&y_{31} = y_3 - y_1, \quad y_{32} = y_3 - y_2, \quad g_1 = d_1y_3 - d_3y_1,\\
&g_2 = d_2y_3 - d_3y_2, \quad M_{23} = M_2y_3 - M_3y_2, \quad M_{13} = M_1y_3 - M_3y_1,\\
&P_{23} = P_2y_3 - P_3y_2,\\
&P_{13} = P_1y_3 - P_3y_1, \quad j_{32} = b_3y_2 - b_2y_3, \quad j_{31} = b_3y_1 - b_1y_3
\end{aligned} \tag{39}$$

Upon expanding the determinant, after lengthy but straightforward algebraic reductions and simplifications, the secular equation (38) can be rewritten as

$$\sinh(\beta h) = \frac{c_{12}(c_{21}c_{33} - c_{31}c_{23}) - c_{11}(c_{22}c_{33} - c_{32}c_{23}) + c_{13}(c_{21}c_{32} - c_{31}c_{22})}{c^*(c_{21}c_{32} - c_{31}c_{22})} \tag{40}$$

where elements c_{ij} are given by

$$\begin{aligned}
&c_{i1} = b_{24}(b_{j1}b_{15} - b_{11}b_{j5}) + b_{11}b_{25}b_{j4}, \quad j = 3,4,5, \ \ i = j-2\\
&c_{i2} = b_{24}(b_{j2}b_{15} - b_{j5}b_{12}) + b_{j4}(b_{22}b_{15} - b_{25}b_{12}), \quad j = 3,4,5,\\
&\quad i = j-2\\
&c_{13} = b_{24}b_{13}b_{35} - b_{34}(b_{23}b_{15} - b_{25}b_{13}),\\
&c_{i3} = b_{24}(b_{j3}b_{15} - b_{j5}b_{13}) - b_{j4}(b_{23}b_{15} - b_{25}b_{13}), \quad j = 4,5,\\
&\quad i = j-2\\
&c^* = b_{24}b_{33}b_{45}
\end{aligned} \tag{41}$$

The quantities b_{ij} are defined as

$$\begin{aligned}
&b_{11} = a_{31}, \quad b_{12} = a_{27}a_{16}f_5 + f_1f_4, \quad b_{13} = a_{27}a_{16}f_6 + f_2f_4,\\
&b_{15} = a_{27}a_{16}f_7 + f_3f_4, b_{22} = a_{27}f_8 - a_{47}f_1, \quad b_{23} = a_{27}f_9 - a_{47}f_2,\\
&b_{24} = \frac{a_{44}}{a_{16}}, \quad b_{25} = a_{27}f_{10} - a_{47}f_3\\
&b_{i1} = a_{j1}, \quad b_{i2} = a_{16}a_{17}a_{27}a_{j2} + a_{17}a_{j6}f_1, \quad j = 5,6,7, \ \ i = j-2,\\
&b_{33} = a_{16}a_{17}a_{27}a_{53} + \left\{\frac{a_{17}a_{56}}{\sinh(\beta h)}\right\}f_2, \quad b_{43} = a_{16}a_{17}a_{27}a_{63} + a_{17}a_{66}f_2,\\
&b_{53} = a_{17}a_{76}f_2\\
&b_{i4} = a_{j4}, \quad b_{i5} = a_{16}a_{17}a_{27}a_{j5} + a_{17}a_{j6}f_3, \quad j = 5,6,7, \ \ i = j-2
\end{aligned} \tag{42}$$

where

$$\begin{aligned}
&f_1 = a_{22}a_{17} - a_{27}a_{12}, \quad f_2 = a_{23}a_{17} - a_{27}a_{13},\\
&f_3 = a_{25}a_{17} - a_{27}a_{15}, \quad f_4 = a_{36}a_{17} - a_{16}a_{37},\\
&f_5 = a_{32}a_{17} - a_{12}a_{37}, \quad f_6 = a_{33}a_{17} - a_{13}a_{37},\\
&f_7 = a_{35}a_{17} - a_{15}a_{37}, \quad f_8 = a_{42}a_{17} - a_{12}a_{47},\\
&f_9 = a_{43}a_{17} - a_{13}a_{47}, \quad f_{10} = a_{45}a_{17} - a_{15}a_{47}
\end{aligned}$$

The complex transcendental secular equation (40) contains complete information about the phase velocity, wave number,

attenuation coefficient and specific loss factor of the waves traveling at the interface which are also known as interfacial guided waves.

5. Solution of secular equation

In general, wave number and hence the phase velocities of the waves are complex quantities, therefore the waves are attenuated in space. In order to solve the secular equation (40), we take

$$c^{-1} = V^{-1} + i\omega^{-1}Q \tag{43}$$

where $k = R + iQ,\ R = \frac{\omega}{V}$, and R, Q are real numbers. Here, it may be noted that V and Q, respectively, represent the phase velocity and attenuation coefficient of the waves. Using representation (43) in various relevant relations, the complex roots $m_i^2\ (i = 1,2,3)$ can be computed from Eq. (28) with the help of Cardano method. The roots m_i^2 are further used to solve secular equation (40) to obtain phase velocity (V) and attenuation coefficient (Q) of the surface waves by using function iteration numerical technique outlined below:

In general the secular equation (40) is of the form $c = \phi(c)$ which on using representation (43) leads to a system of two real equations $f(V,Q) = 0$ and $g(V,Q) = 0$. In order to apply functional iteration method we write $V = f^*(V,Q)$ and, $Q = g^*(V,Q)$ where the functions f^* and $g^*$are selected in such a way that they satisfy the conditions

$$\left|\frac{\partial f^*}{\partial V}\right| + \left|\frac{\partial f^*}{\partial Q}\right| < 1, \qquad \left|\frac{\partial g^*}{\partial V}\right| + \left|\frac{\partial g^*}{\partial Q}\right| < 1 \tag{44}$$

for all V, Q in the neighborhood of the root. If (V_0, Q_0) be an initial approximation to root, then we can construct the successive approximations according to the formulae

$$\begin{aligned} V_1 &= f^*(V_0, Q_0), \qquad Q_1 = g^*(V_1, Q_0) \\ V_2 &= f^*(V_1, Q_1), \qquad Q_2 = g^*(V_2, Q_1) \\ &\vdots \qquad\qquad\quad \vdots \\ V_{n+1} &= f^*(V_n, Q_n), \quad Q_{n+1} = g^*(V_{n+1}, Q_n) \end{aligned} \tag{45}$$

The sequence (V_n, Q_n) of approximations to the root will converge to the actual root provided (V_0, Q_0) lies in the neighborhood of the actual root. For initial value of $c = c_0 = (V_0, Q_0)$, the roots $m_i\ (i = 1,2,3)$ are computed from Eq. (28) by using Cardano method for each value of the non-dimensional wave number (R) for assigned frequency. The values of m_i so obtained are then used in secular equation (40) to obtain the current values of V and Q each time which are further used to generate the sequence (45). The process is terminated as and when the condition $|V_{n+1} - V_n| < \varepsilon$, ε being arbitrarily small number to be selected at random to achieve the accuracy level, is satisfied. The procedure is continuously repeated for different values of non-dimensional wave number (R) to obtain corresponding values of the phase velocity (V) and attenuation coefficient (Q). Thus, the real phase velocity and attenuation coefficient during the propagation of Rayleigh type waves in the composite structure under study can be computed from dispersion relation (40).

5.1. Specific loss

According to Kolsky (1963), in case of sinusoidal plane wave of small amplitude, the specific loss $\frac{\Delta W}{W}$ equals to 4π times the ratio of absolute value of the imaginary part of k to the real part of k, i.e. $\frac{\Delta W}{W} = 4\pi\left|\frac{Im(k)}{Re(k)}\right|$, where k is a complex number such that $Im(k) > 0$. Here

$$\frac{\Delta W}{W} = 4\pi\left|\frac{Im(k)}{Re(k)}\right| = 4\pi\left|\frac{Q}{R}\right| = 4\pi\left|\frac{VQ}{\omega}\right| \tag{46}$$

6. Special cases of wave solution

In case the semiconductor layer is absent ($h = 0$), then the composite structure reduces to a piezoelectric halfspace subject to stress free, open circuit/closed circuit boundary conditions. The secular equation (40) and hence (38) in this case reduces to following two equations:

$$y_1(d_2b_3 - d_3b_2) - y_2(d_1b_3 - d_3b_1) + y_3(d_1b_2 - d_2b_1) = 0 \tag{47}$$

$$y_1(d_2P_3 - d_3P_2) - y_2(d_1P_3 - d_3P_1) + y_3(d_1P_2 - d_2P_1) = 0 \tag{48}$$

where y_i, d_i, b_i and $P_i\ (i = 1,2,3)$ are defined in Eqs. (37) and (30).

Eq. (47) corresponds to the secular equation which governs the surface wave motion in case of stress free and open circuit (OC) boundary conditions prevailing at the surface of piezoelectric halfspace, and Eq. (48) refers to the secular equation for stress free and closed circuit (CC) surface of the piezoelectric halfspace.

Table 1
Physical data of 6 mm class cadmium selenide (CdSe) and lead zirconate titanate (PZT-4) piezoelectric materials (Sharma and Pal, 2004; Wang and Quek, 2002).

S. No.	Quantity	Unit	CdSe	PZT-4
1	ρ^p	kg m^{-3}	5.504×10^3	7.5×10^3
2	c_{11}	GPa	74.41	132.0
3	c_{13}	GPa	39.30	73.0
4	c_{33}	GPa	83.60	115.0
5	c_{44}	GPa	13.20	26.0
6	e_{31}	C m^{-2}	−0.160	−4.1
7	e_{33}	C m^{-2}	0.347	14.1
8	e_{15}	C m^{-2}	−0.138	10.5
9	ε_{11}	ε_0	9.329	801.90
10	ε_{33}	ε_0	10.198	655.10
11	ε_0	farads/m	8.854×10^{-12}	8.854×10^{-12}

Table 2
Physical data of n-type silicon (Si) and germanium (Ge) semiconductors (Sharma and Thakur, 2006; Maruszewski, 1989).

S. No.	Quantity	Unit	Si	Ge
1	ρ^s	kg m^{-3}	2.3×10^3	5.3×10^3
2	λ	GPa	64.0	48.0
3	μ	GPa	65.0	53.0
4	D^n	m^2 s^{-1}	0.35×10^{-2}	1×10^{-2}
5	n_0	m^{-3}	10^{20}	10^{20}
6	α_T	K^{-1}	2.6×10^{-6}	5.8×10^{-6}

Table 3
Phase velocity for first mode at two different life times in semiconductor–piezoelectric composites.

Wave number	Si–CdSe		Ge–CdSe		Ge–PZT	
Rh	1 ps	0.1 ps	1 ps	0.1 ps	1 ps	0.1 ps
0.01	234.65	210.08	234.28	212.62	231.13	207.46
0.05	46.93	42.007	46.66	42.54	46.23	41.49
0.1	23.35	20.989	23.33	21.24	23.13	20.74
1.0	2.387	2.103	2.374	2.099	2.376	2.097
2.0	1.257	1.127	1.253	1.071	1.254	1.128
3.0	0.915	0.813	0.873	0.776	0.916	0.837
4.0	0.772	0.676	0.778	0.676	0.779	0.714
5.0	0.708	0.617	0.722	0.631	0.726	0.661
6.0	0.678	0.617	0.663	0.630	0.663	0.589
7.0	0.648	0.617	0.632	0.603	0.649	0.562
8.0	0.633	0.607	0.618	0.595	0.588	0.513
9.0	0.633	0.583	0.594	0.562	0.570	0.513
10.0	0.619	0.582	0.590	0.550	0.567	0.501

7. Numerical results and discussion

To illustrate the analytical developments in the previous section, we now perform some numerical simulations. In order to explore the effect of different interacting fields and life times of carriers on the phase velocity, attenuation coefficient and specific loss of the waves, the secular equation (40) pertaining to the analytical model under consideration is solved numerically for three composite strictures namely: (i) Si–CdSe composite, (ii) Ge–CdSe composite, and (iii) Ge–PZT composite.

The physical data for piezoelectric halfspace and semiconductor layer is given in Tables 1 and 2, respectively. The numerical computations have been performed by employing the procedure outlined in Section 5 with the help of MATLAB programming. Due to the closeness of results and hence in order to avoid clustering of profiles in the graphs, the computer simulated values of phase velocity and attenuation coefficient of first mode of wave propagation corresponding to two life times $t_n^+ = 0.1$ ps and $t_n^+ = 1$ ps are given in Tables 3 and 4 for comparison purpose, respectively.

In the following discussion, *Rh* denotes non-dimensional wave number of the waves traveling at the interface of layer and halfspace while *R* represents the wave number of Rayleigh surface waves at free surface of piezoelectric halfspace.

The close inspection of various values of phase velocity and attenuation coefficient in Tables 3 and 4 reveals that the computer simulated results for the considered choices of patch and core materials in the composites are in close agreement at different wavelengths and life times of the charge carriers in semiconductor materials. It is clear from the tabulated values that both phase velocity and attenuation coefficient increase with increasing life time of the carriers in Si–CdSe, Ge–CdSe and Ge–PZT composites. However, the magnitude of attenuation coefficient is quite small in case of Ge–CdSe and Ge–PZT composites at long wavelengths as compared to that in Si–CdSe composite. This means that the wave signals travel longer distances in composites having patch of germanium (Ge) semiconductor than those with silicon (Si) patch. The trends of physical parameters at short wavelengths $Rh \geqslant 1$ are comparable in magnitude for all the composites. The profiles of phase velocity (*V*), attenuation coefficient (*Q*) and specific loss factor (*SL*) of first three modes of wave propagation in Si–CdSe composite are plotted with respect to the non-dimensional wave number at $t_n^+ = 1$ ps in Figs. 2–4 for illustration and

Table 4
Attenuation coefficient for first mode at two different life times in semiconductor–piezoelectric composites.

Wave number	Si–CdSe		Ge–CdSe		Ge–PZT	
Rh	1 ps	0.1 ps	1 ps	0.1 ps	1 ps	0.1 ps
0.01	0.000185	0.000149	0.000067	0.000051	0.000099	0.000061
0.05	0.000952	0.000640	0.000380	0.000221	0.000520	0.002401
0.1	0.002069	0.001530	0.001031	0.000530	0.001194	0.000550
1.0	0.049385	0.029900	0.051022	0.022120	0.036233	0.017810
2.0	0.043587	0.016900	0.038999	0.010227	0.029173	0.007010
3.0	0.005894	0.001837	0.020481	0.006376	0.015954	0.004750
4.0	0.029587	0.017100	0.041770	0.021810	0.028880	0.012205
5.0	0.028494	0.001849	0.055814	0.024100	0.024969	0.001310
6.0	0.007678	0.003390	0.008349	0.004010	0.004922	0.001424
7.0	0.263372	0.210434	0.061387	0.512832	0.818264	0.250809
8.0	1.362632	0.997555	1.002845	0.921977	1.916598	0.885914
9.0	2.154704	1.432021	2.203237	1.583276	3.275625	1.093255
10.0	3.123673	1.760425	3.687035	2.150000	3.943320	1.196117

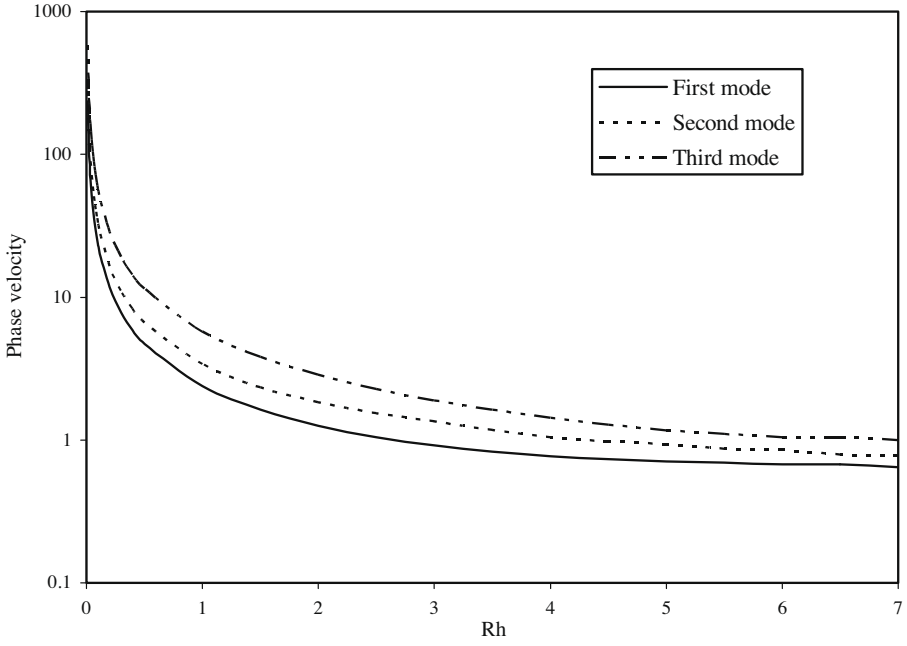

Fig. 2. Variation of phase velocity versus *Rh* in composite for $t_n^+ = 1$ ps.

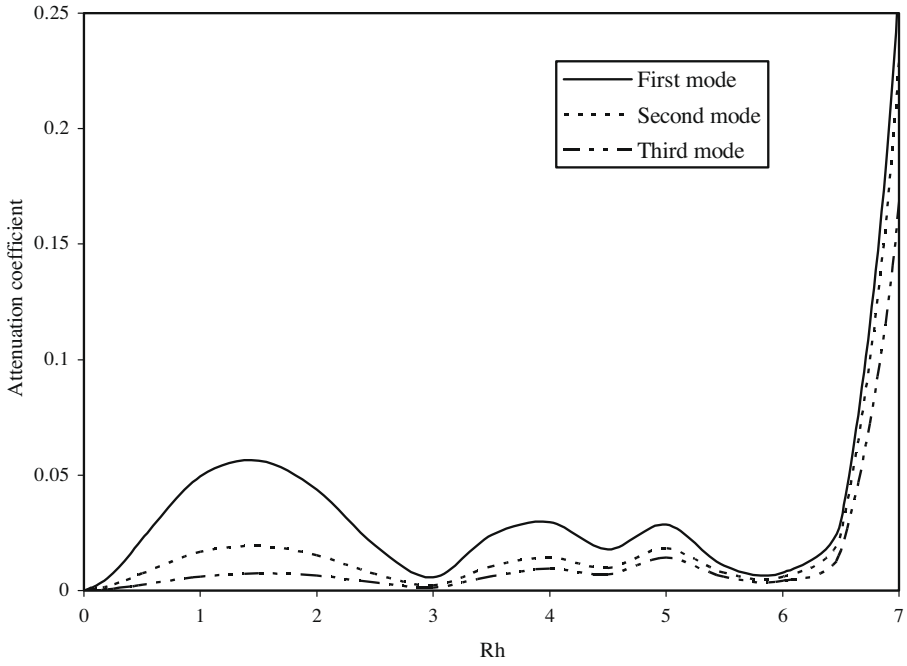

Fig. 3. Variation of attenuation coefficient versus *Rh* in composite for $t_n^+ = 1$ ps.

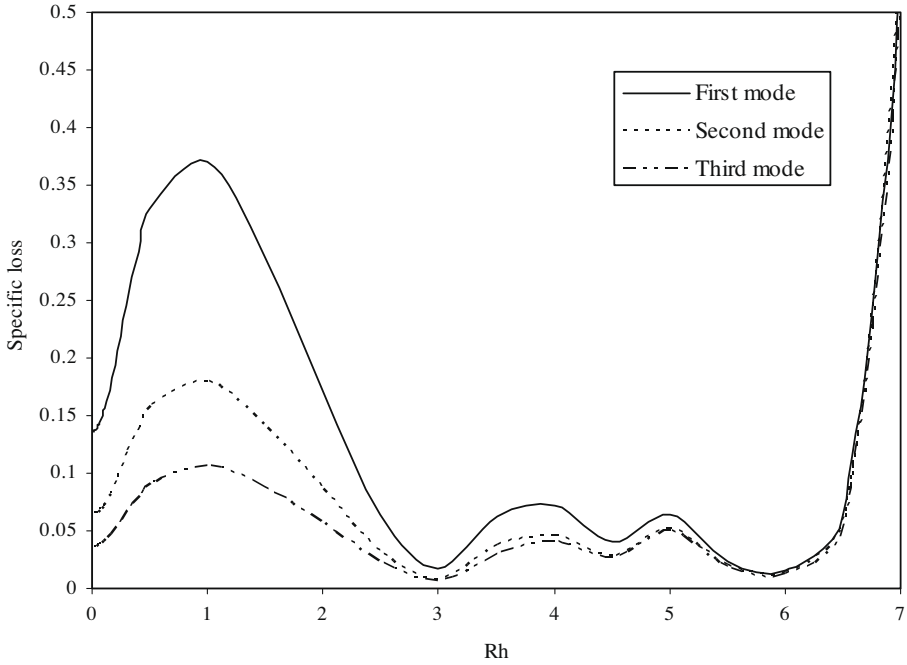

Fig. 4. Variation of specific loss versus *Rh* in composite for $t_n^+ = 1$ ps.

discussion purpose. The phase velocity versus wave number is plotted on linear-log scales in Figs. 2, 5 and 8. The effect of different types of boundary conditions prevailing at the surface of a piezoelectric halfspace is shown in Figs. 5–7. The variation of phase velocity and attenuation coefficient in composite structure with wave number at two values of life time of carriers is presented in Figs. 8, 9. The results in the physical domain can be obtained with the help of quantities defined in Eq. (10) from the instant non-dimensional one.

Fig. 2 shows the variations of phase velocity for the first three modes of wave propagation with the non-dimensional wave number (*Rh*) on linear-log scales in the Si–CdSe composite. It is found that the phase velocity profiles are clearly dispersive in character and attenuating in space. The magnitudes of the phase velocity of all the three modes decreases sharply with increasing wave number (*Rh*) in the range $0 \leqslant Rh \leqslant 1$ and moderately in the interval $1 \leqslant Rh \leqslant 4$ before these become almost steady and uniform for $Rh \geqslant 4$. Initially the phase velocity has large value for the higher modes of wave propagation as compared to that of lower modes.

It is worth noting that all the modes start with the higher phase velocity at long wave lengths and hence shows the cut off frequencies for their appearance/existence. Moreover, the dispersion at

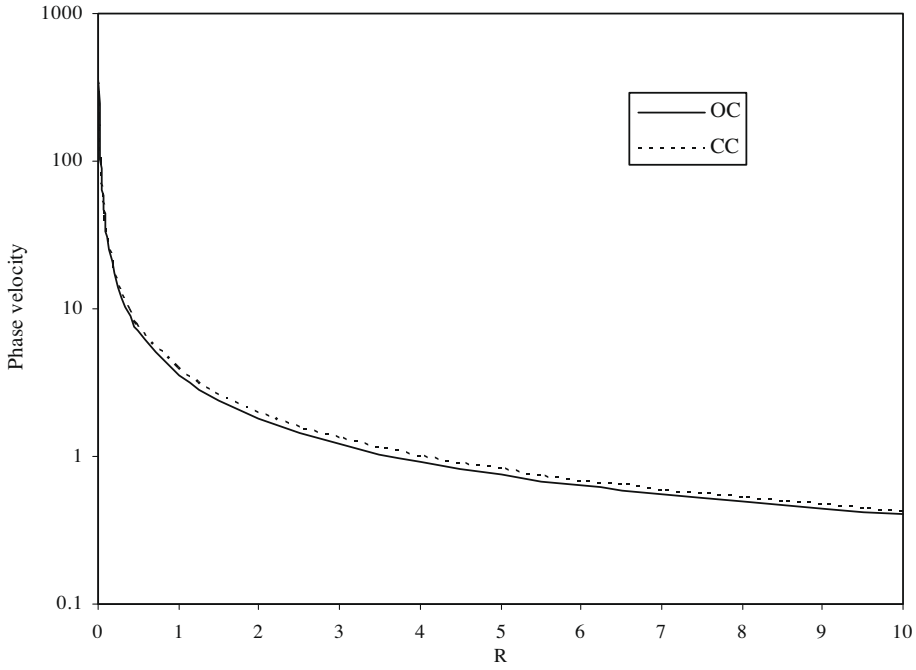

Fig. 5. Variation of phase velocity versus R in piezoelectric halfspace.

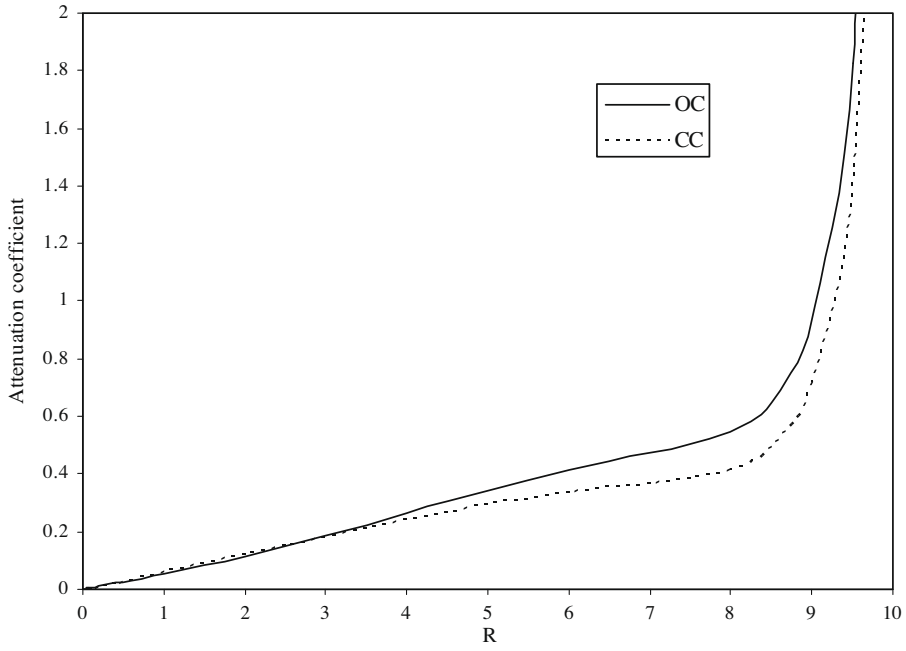

Fig. 6. Variation of attenuation coefficient versus R in piezoelectric halfspace.

long wavelengths has been observed, which is useful for device applications, where long wavelengths (wavelength $\gg$ layer thickness) are preferred. Figs. 3 and 4 present the variations of attenuation coefficient and specific loss factor as a function of wave number (Rh). The variations of attenuation as well as specific loss factor of energy dissipation are nearly oscillatory in the range $0 \leqslant Rh \leqslant 6$ which increase sharply for $Rh \geqslant 6$ for all modes. It is clearly evident from Figs. 3 and 4 that lower modes of interfacial wave have large value of attenuation coefficient as well as specific loss factor as compared to that of higher modes.

Fig. 5 represents the variations of non-dimensional phase velocity versus non-dimensional wave number (R) on linear-log scales in piezoelectric halfspace under open circuit (OC) and closed circuit (CC) surface conditions, in the absence of semiconductor layer ($h \to 0$). It is observed that the magnitude of the phase velocity decreases sharply with wave number in the range $0 \leqslant R \leqslant 1$ and moderately for range $1 \leqslant R \leqslant 5$, before it becomes steady and uniform at $R \geqslant 5$. It is also found that the phase velocity (V_{CC}) for closed circuit boundary condition is slightly higher in magnitude than that for open circuit (V_{OC}) one.

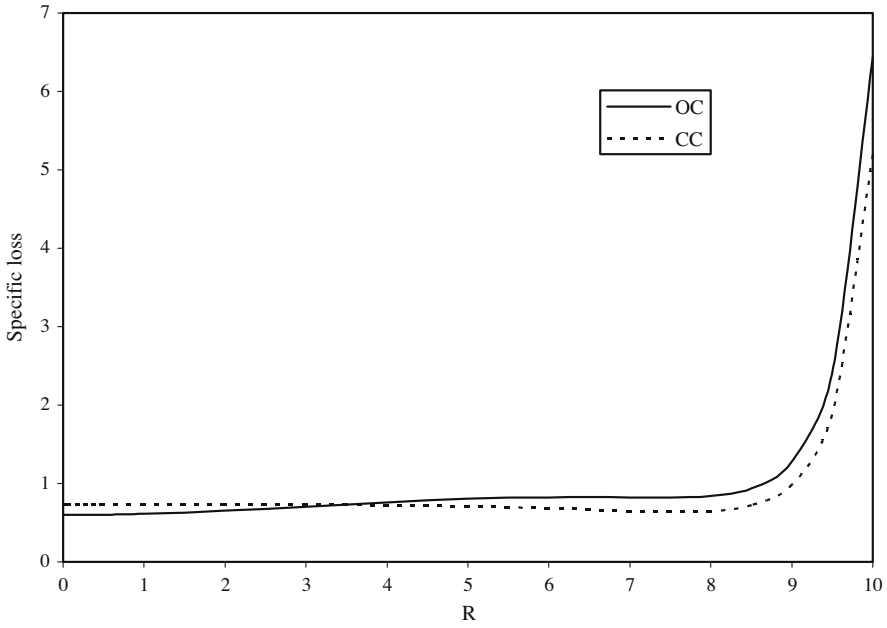

Fig. 7. Variation of specific loss versus R in piezoelectric halfspace.

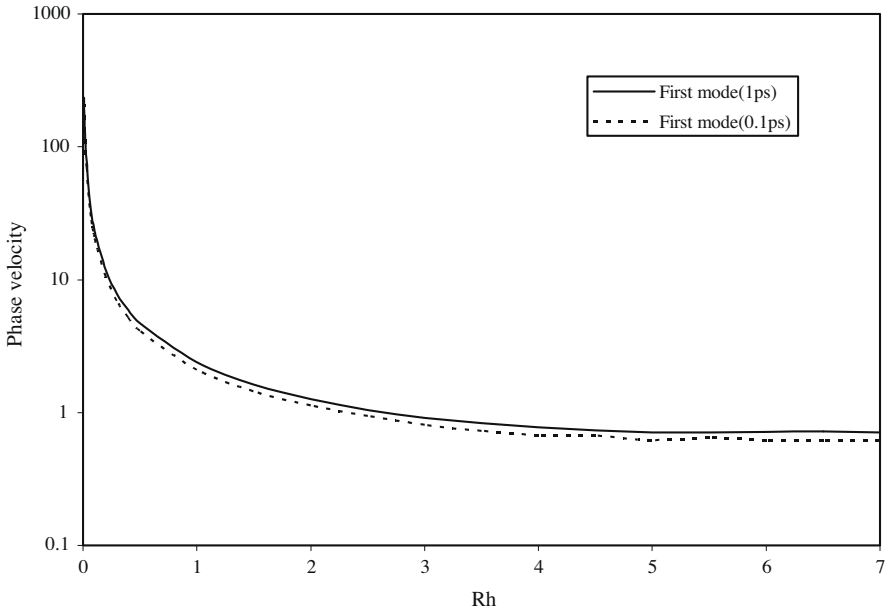

Fig. 8. Variation of phase velocity versus Rh in composite for $t_n^+ = 1, 0.1$ ps.

Fig. 6 shows the variations of attenuation coefficient with wave number (R) in case of OC and CC boundary of the halfspace when $h \to 0$. The profiles of attenuation coefficient increase monotonically in a steady manner for $0 \leqslant R \leqslant 8.5$. However, these profiles are sharply increased for $R \geqslant 8.5$ in both boundary conditions. Moreover, the attenuation Q_{OC} in case of open circuit is slightly less than that of closed circuit Q_{CC} for $0 \leqslant R \leqslant 3$ and this trend is reversed for $R \geqslant 3$. Fig. 7 shows the variation of specific loss factor of energy dissipation as a function of wave number (R) for OC and CC boundaries of the piezoelectric halfspace in the absence of semiconductor layer ($h \to 0$). It is evident that the specific loss SL_{CC} for closed circuit boundary possesses almost uniform behavior whereas specific loss SL_{OC} in case of open circuit increases moderately with increasing wave number and it interlace according to $SL_{OC} < SL_{CC}$ for $0 \leqslant R \leqslant 3.0$ and this trend get reversed beyond $R \geqslant 3$. The profiles of this physical quantity corresponding to OC and CC boundary conditions experience sharp increase in their magnitude for $R \geqslant 8.5$.

Fig. 8 shows the variations of phase velocity with wave number for first mode of wave propagation in the Si–CdSe composite at carrier life time $t_n^+ = 1$ ps and $t_n^+ = 0.1$ ps. Here also it is evident that the magnitude of phase velocity is slightly higher for life time $t_n^+ = 1$ ps than that at $t_n^+ = 0.1$ ps, though the basic behavior of the phase velocity profiles remains the same. Fig. 9 shows the variations of attenuation coefficient for first mode of wave propagation with the non-dimensional wave number in Si–CdSe structure at

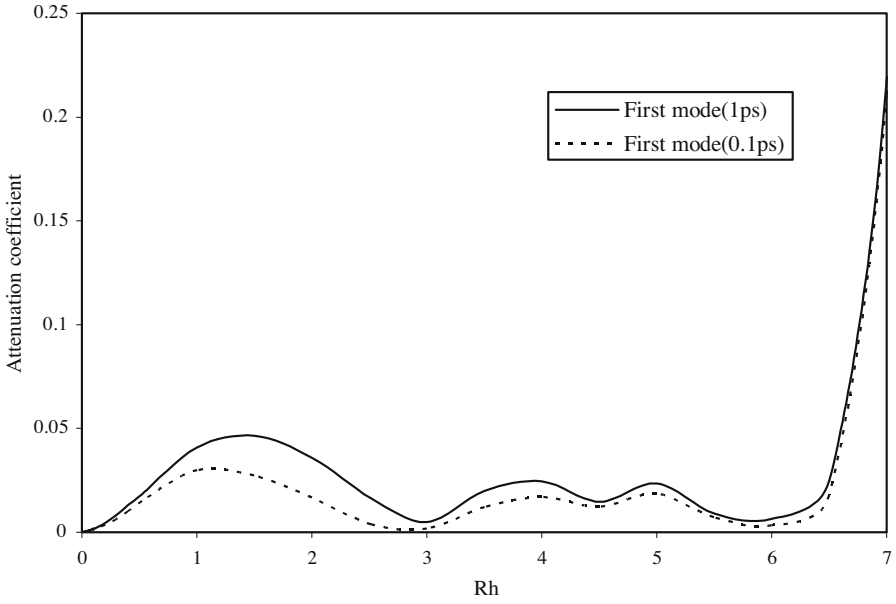

Fig. 9. Variation of attenuation coefficient *Rh* in composite $t_n^+ = 1, 0.1$ ps.

$t_n^+ = 1$ ps and $t_n^+ = 0.1$ ps. It is observed that the attenuation is higher for $t_n^+ = 1$ ps than that at $t_n^+ = 0.1$ ps, though the profiles are similar.

From Figs. 2–9 it can be concluded that the characteristics of interfacial waves in the Si–CdSe composite are greatly influenced by life times of carriers and thickness of the semiconductor patch applied on the piezoelectric (CdSe) core material. Similar type of conclusion can be drawn in cases of Ge–CdSe and Ge–PZT composites which is also evident from simulation data reported in Tables 3 and 4. It is worth reporting here that the replacement of core material CdSe with PZT under germanium (Ge) patch results in reduction of phase velocity, however, it slightly increases the attenuation of waves propagating at the interface of the composites.

8. Conclusions

In the present study, the functional iteration numerical technique along with Cardano method has been successfully employed to solve complex secular equations in order to obtain the phase velocities, attenuation coefficients and specific loss factors of energy dissipation. The propagating waves in the considered composite structure are dispersive in nature. Phase velocity in Si–CdSe, Ge–CdSe and Ge–PZT composites has been noticed to decrease sharply at long wavelengths and possess almost uniform and stable behavior at short wavelengths as in case of piezoelectric halfspace. The oscillatory nature of attenuation coefficient and specific loss factor for these composites has been observed at large wavelengths and after a specific value of the wave number these physical parameters are sharply increased. However, in case of piezoelectric halfspace at small values of wave number, the specific loss factor first assumes almost uniform behavior and then it increases with the wave number for both open and closed circuit boundary conditions. In contrast the profiles of attenuation coefficient show monotonically increasing trend. Moreover, with increasing degree of harmonics the attenuation and specific loss factor decreases and reverse trend follows for the phase velocity in these composite structures. The phase velocity and attenuation coefficient also increases with life time of carriers for all three structures. From the comparative analysis presented in tabular form for all three composites, we conclude that the interfacial wave signals can travel longer distances in composites having patch of germanium (Ge) semiconductor in comparison to those with silicon (Si) patch. Significant modifications of the wave characteristics have been noticed due to the application of semiconductor patches at the surface of the piezoelectric halfspace in contrast to free conditions prevailing on it. The study may find applications in SAW devices and electronics industry.

Acknowledgements

The authors are thankful to the reviewers for their deep interest and useful suggestions for the improvement of this work.

References

Chen, T.Y., 1971. Further correspondences between plane piezoelectricity and generalized plane strain elasticity. Proceedings of Royal Society of London A 454, 873–884.

Chizhikov, S.I., Sorokin, N.G., Petrakov, V.S., 1985. The elastoelectric effect in the non-centrosymmetric crystal. In: Taylor, G.W. et al. (Eds.), Piezoelectricity. Gordon & Breach Science Publishers, New York, pp. 5–91.

Collins, J.H., Lakin, K.M., Quate, C.F., Shaw, H.J., 1968. Amplification of acoustic surface waves with adjacent semiconductor and piezoelectric crystals. Applied Physics Letters 13, 314–316.

Curie, J., Curie, P., 1880. Development par compression de l'etricite polaire das les cristaux hemledres a faces inclines. Bulletin No. 4 de la Societee Minearalogique de France, p. 3.

de Lorenzi, H.G., Tierten, H.F., 1975. On the interaction of the electromagnetic field with heat conducting deformable semiconductors. Journal of Mathematical Physics 16, 938–957.

Dietz, D.R., Busse, L.J., Fife, M.J., 1988. Acoustoelectric detection of ultrasound power with composite piezoelectric and semiconductor devices. IEEE Transactions on Ultrasonics, Ferroelectrics and Frequency Control 35, 146–151.

Fischler, C., 1970. Acoustoelectric amplification in composite piezoelectric and semiconducting structures. IEEE Transactions on Electron Devices 17, 214–218.

Fischler, C., Yando, S., 1969. Amplification of guided elastic waves in piezoelectric plates through electrical coupling to a semiconductor. Applied Physics Letters 15, 366–368.

He, J.H., 2001. Coupled variational principles of piezoelectricity. International Journal of Engineering Science 39, 323–341.

Hutson, A.R., White, D.L., 1962. Elastic wave propagation in piezoelectric semiconductors. Journal Applied Physics 33, 40–47.

Kino, G.S., Reeder, T.M., 1971. A normal mode theory for the Rayleigh wave amplifier. IEEE Transactions on Electron Devices 18, 909–920.

Kolsky, H., 1963. Stress Waves in Solids. Dover Press, New York.

Maruszewski, B., 1989. Thermodiffusive surface waves in semiconductors. Journal of Acoustic Society of America 85, 1967–1977.

Maugin, G.A., Daher, N., 1986. Phenomenological theory of elastic semiconductors. International Journal of Engineering Science 24, 703–731.
Sharma, J.N., Pal, M., 2004. Propagation of lamb waves in a transversely isotropic piezothermoelastic plate. International Journal of Sound and Vibration 270, 587–610.
Sharma, J.N., Thakur, N., 2006. Plane harmonic elasto-thermodiffusive waves in semiconductor materials. Journal of Mechanics of Materials and Structures 1, 813–835.
Sharma, J.N., Walia, V., 2007. Further investigations on Rayleigh waves in piezothermoelastic materials. International Journal of Sound and Vibration 301, 189–206.
Sharma, J.N., Pal, M., Chand, D., 2005. Propagation characteristics of Rayleigh waves in transversely isotropic piezothermoelastic materials. International Journal of Sound and Vibration 284, 227–248.
Sharma, J.N., Thakur, N., Singh, S., 2007. Propagation characteristics of elasto-thermodiffusive surface waves in semiconductor material half-space. Journal of Thermal Stresses 30, 357–380.
Sharma, J.N., Sharma, I., Chand, S., 2008. Elasto-thermodiffusive surface waves in a semiconductor half-space underlying a fluid with varying temperature. Journal of Thermal Stresses 31, 956–975.
Sharma, J.N., Thakur, N., Singh, S., 2009. Elasto-thermodiffusive (ETNP) surface waves in semiconductor materials. International Journal of Solids and Structures 46, 2309–2319.
Wang, J.J., Quek, S.T., 2002. Lamb wave propagation in a metallic semi-infinite medium covered with piezoelectric layer. International Journal of Solids and Structures 39, 2547–2556.
Weinreich, G., Sanders Jr., T.M., White, H.G., 1959. Acoustoelectric effect in n-type germanium. Physics Review 114, 33–44.
White, D.L., 1962. Amplification of ultrasonic waves in piezoelectric semiconductors. Journal of Applied Physics 33, 2547–2554.
White, R.M., 1967. Surface elastic-wave propagation and amplification. IEEE Transactions on Electron Devices 14, 181–189.
Yang, J.S., Zhou, H.G., 2004. Acoustoelectric amplification of piezoelectric surface waves. Acta Machanica 172, 113–122.
Yang, J.S., Zhou, H.G., 2005. Amplification of acoustic waves in piezoelectric semiconductor plates. International Journal of Solids and Structures 42, 3171–3183.